NASA TECHNICAL MEMORANDUM

NASA TM X-68205

NASA TM X-68205

THEORETICAL AND EXPERIMENTAL INVESTIGATION OF THE NONLINEAR BEHAVIOR OF ANGLEPLIED BORON/ALUMINUM COMPOSITES

by C. C. Chamis and T. L. Sullivan
Lewis Research Center
Cleveland, Ohio 44135

TECHNICAL PAPER proposed for presentation at
Third Symposium on Composite Materials: Testing and Design sponsored by the American Society for Testing and Materials
Williamsburg, Virginia, March 19-23, 1973

THEORETICAL AND EXPERIMENTAL INVESTIGATION OF THE NONLINEAR BEHAVIOR OF ANGLEPLIED BORON/ALUMINUM COMPOSITES

by C. C. Chamis* and T. L. Sullivan*

Lewis Research Center

ABSTRACT

Specimens from angleplied laminates of boron/aluminum composites were tested and the results analyzed. The specimens consisted of eight-ply symmetric layups $(0_2, \pm\theta)_s$ and were loaded in tension at various angles to the 0^o-ply direction. Stress-strain curves to specimen fracture were obtained. The analysis was performed using linear composite mechanics which includes residual stresses and a combined stress yield function. The results obtained indicate that angleplied boron/aluminum laminates exhibit a nonlinear stress-strain behavior to fracture. The residual stresses affect the initial and "yield" laminate properties. Linear composite mechanics is inadequate to predict the mechanical behavior of boron/aluminum angleplied laminates.

Key Words: Boron/aluminun composites; Angleplied laminates; Stress-strain curves; Yield stress; Fracture stress; Residual stress; Linear composite mechanics; Nonlinear stress-strain behavior.

E-7378

---

*Aerospace Engineer.

SYMBOLS

E	normal modulus (Youngs, extensional)
F	combined stress yield or limit function
G	shear modulus
S	strength (subscripts denote plane, direction, and sense)
T	temperature
α	coefficient thermal of expansion
ϵ	strain
θ	ply orientation angle
$\theta_{L/O}$	load direction angle with respect to the 0^{O}-ply direction
ν	Poisson's ratio
σ	stress

Subscripts:

C, c	compression, composite or laminate property
l	ply property
m	matrix property
S, s	shear, symmetry
T	tension
x, y	laminate structural axes directions
1, 2	ply orthotropic axes directions

INTRODUCTION

Feasibility studies for the application of fiber composites to systems such as the space shuttle and turbine engines have indicated that boron/aluminum composites are leading contenders as primary struc-

tural materials. Boron/aluminum composites offer distinct advantages over nonmetallic-matrix composites in elevated temperature applications (400° to 700° F) and in moist, erosive, and other environments.

Unidirectional composites of boron/aluminum have been extensively characterized (1, 2, 3)[1] experimentally for loadings parallel to and at various angles to the fiber direction. However, a combined experiment/theory systematic study to investigate the mechanical behavior of boron/aluminum angleplied composites has been lacking.

For this reason, a combined experiment/theory investigation was conducted with the following objectives:

1. Characterize the mechanical behavior of boron/aluminum angleplied laminates experimentally.

2. Compare predicted results, based on the properties of the unidirectional laminate, with measured data and thereby determine the applicability and/or limitation of linear composite mechanics to angleplied boron/aluminum composites.

3. Assess the influence of lamination residual stresses on the initial linear portion of the stress/strain curve of the angleplied laminates.

4. Obtain an assessment of the strength of the individual plies within the angleplied boron/aluminum composite.

EXPERIMENTAL INVESTIGATION

Material, Test Apparatus, and Procedure

Using 0.004 inch boron fiber and 6061-O aluminum foil, composite plates 12 inches square were fabricated by a supplier using conventional diffusion bonding process. Fiber volume was approximately 50 percent. The laminate configurations were of the form $(0_2^{\circ}, \pm\theta^{\circ})_S$, or $(0 \pm \theta)_S$ for writing convenience, where θ was 0°, 5°, 15°, 30°, 45°, and 90°, figure 1. Coupons were cut at various angles from the plates by shearing.

[1]The numbers in parentheses refer to list of references appended to this paper.

The sheared edges were then ground with a diamond wheel to produce a coupon width of 0.500. Coupon length was 10 inches. Results reported herein concern tests of coupons where the load angle with respect to the 0°-ply was $\theta_{L/O} = 0^{\circ}$ for all six laminate configurations and $\theta_{L/O} = 10^{\circ}$, 15°, and 30° for two ply laminate configurations, $\theta = 15^{\circ}$ and 30°.

The six coupons where $\theta_{L/O} = 0^{\circ}$ had their ends reinforced with aluminum tabs. The other six were not reinforced. Each coupon was instrumented with strain gage rosettes as shown in figure 2. The coupons were clamped in serated, bolted grips and loaded to failure in a hydraulic universal testing machine. The grips are shown in figure 3. Loading was halted at intervals for acquiring strain gage data on a digital strain recorder.

Test Results

Stress strain curves for each coupon test are plotted in figures 4 to 6. Experimental data are tabulated in table I. Strain values were obtained from the rosette at the coupon center (gage 2). The other strain gages were used to determine the strain gradient across the width and the end effects. However, data from these gages are not relevant to the present objectives and will not be discussed further.

The unidirectional specimen ($\theta = \theta_{L/O} = 0^{\circ}$) initially failed at a stress much less than that expected. However, examination of the fracture surface revealed a misalined fiber (fig. 7). Since the fracture occurred near the grip, it was possible to retest this specimen. The specimen was reloaded and this time it failed at a stress about 25 percent greater than the initial failure stress.

For coupons where $\theta_{L/O}$ was less than or equal to θ, failure strain was a nearly constant 0.7 percent. Once $\theta_{L/O}$ exceeded θ, failure strain increased substantially. For the tests $\theta_{L/O} \leq \theta$ some of the fibers were coincident or within small angles from the load direction.

THEORETICAL INVESTIGATION

Linear Laminate Analysis

The test specimens were analyzed using linear laminate analysis. The analysis consisted of calculating (1) the initial and final (fracture load) elastic constants and (2) the ply stresses at the yield load and at fracture load. The yield load ply stress calculations include the effect of lamination residual stresses.

The linear laminate theory used in the calculations is that available in the NASA Lewis composites computer code (4). Application of linear laminate theory to boron/aluminum composites and a yield criterion are described in (3). Calculation of lamination residual stresses is described in (5). The computer code (4) has capabilities for computing ply lamination residual stresses and ply yield stresses. The ply yield stresses are based on a yield criterion derived using a modified distortion energy principle (3).

Initial and Final Elastic Constants

The unidirectional composite (laminate) properties were supplied by the laminate fabricator table II, column 1. Columns 2 to 4 in table II, were theoretically calculated to obtain an indication of the possible matrix nonlinearity effects on the elastic and thermal constants of the unidirectional composite. The initial laminate properties for the various test specimens were calculated as follows:

1. Typical boron fiber and 6061-O aluminum alloy properties were used as input into the micromechanics parts of the computer code (4).

2. The correlation coefficients in the micromechanics part were adjusted until the predicted values for the unidirectional laminate agreed with those supplied by the fabricator.

3. The values for the correlation coefficients obtained in step 2 above were used as input to the laminate analysis.

The aforementioned approach was taken so that micromechanics could be used to calculate the final elastic constant of the unidirectional composite and the angleplied laminates. The variation of the unidirectional composite properties for progressively decreasing values of the aluminum matrix modulus with increasing strain are tabulated in table II. It is readily observed in table II that the unidirectional laminate transverse mechanical properties decrease very rapidly as the aluminum matrix modulus decreases. Conversely, the mechanical properties along the fiber direction are not as sensitive to matrix modulus variations.

The final elastic constants of the test specimens (properties at fracture load) were calculated by assuming the matrix modulus had a value of 10^5 psi (table II, column 3). This value was selected for the following reason. The test specimens fractured at a laminate strain of about 0.7 percent when some of the ply orientation angles (fiber directions) were parallel with the load direction or nearly so. This means that the strain in the aluminum matrix along the fiber direction was at least 0.7 percent. Available stress-strain curves of the 6061-O aluminum alloy show that the modulus at 0.7 percent strain is about 200 000 psi. The predicted initial and final elastic constants of the test specimens are summarized in table III.

Yield and Fracture Load Ply Stresses

The stresses and loads at yield and at fracture of the test specimens are summarized in table IV. The ply yield stresses were computed by using the unidirectional laminate elastic constants and the observed yield load as inputs to the computer code (4). The yield load was taken to be that load which produced the first observable deviation from the initial linear portion of the specimen stress-strain curve (see figs. 3 to 5). The fracture load ply stresses were computed by using the final unidirectional composite elastic constants (table II, column 3), and the fracture load in the computer code.

Two sets of calculations were performed for the ply yield stresses. The first set included the lamination residual stresses. In the second

set, the lamination residual stresses were omitted. A temperature difference of 900° F was used in the lamination residual stress calculations. The processing temperature for making the laminates was reported by the material supplier to be about 970° F.

The two sets of calculations for the ply yield stresses provide indirect estimates of:

1. The effect of lamination residual stress on the ply yield stress
2. The insitu ply yield strength.

The fracture load ply stress calculations provide a first approximation to estimate the ply longitudinal fracture strength (the fracture strength along the fiber direction).

The calculated ply stresses are summarized in table V for specimens loaded parallel to the 0° ply direction and in table VI for specimens loaded at angles 10°, 15°, and 30° to the 0° ply direction. The corresponding values of the combined stress yield function F is also given in tables IV and V under the yield load ply stresses.

COMPARISONS AND DISCUSSION OF RESULTS

Comparisons of predicted and measured data, the influence of residual stress on the ply yield stress, in situ ply strength, limitations of the linear laminate theory and possible factors contributing to nonlinear composite behavior are discussed in this section.

Comparison of Predicted and Experimental Data

Predicted and experimental values for modulus and Poisson's ratio are summarized in table VII for all the test specimens. Values are given for both initial and final properties. By comparing predicted and experimental values in table VII, it is observed that:

1. The predicted initial values for modulus are in good agreement with the experimental values only for the test specimens of ply orientation $8(0)$ or $(0_2 \pm 5)_s$. The values for the other specimens differ significantly,

from 10 to 70 percent. The predicted values are greater than the experimental values in all cases.

2. The final values for modulus also differ significantly. The predicted values are greater than the experimental values varying anywhere from 10 to 100 percent.

3. The predicted initial values for Poisson's ratio are within 10 percent of the experimental values for all the specimens except the $(0_2, 90_2)_s$ specimen.

4. A wide disparity exists between the final values for Poisson's ratios for the majority of the specimens. Predicted values even have signs opposite to the experimental ones for some cases.

The following two conclusions are made from these observations:

1. The matrix contribution to the initial modulus of the specimens is considerably less than assumed in the calculations. This indicates that the lamination residual stress values are probably stressing the in situ aluminum matrix beyond its 0.2 percent offset strain.

2. Linear laminate theory, as used herein, is not suitable for predicting final properties of angleplied boron/aluminum laminates.

Influence of Lamination Residual Stresses on Yield Load Ply Stresses

It was mentioned previously that the lamination residual stress effects on the in situ ply yield stress can be estimated by calculating the yield load ply stresses with and without residual stress. Recall that the yield load was taken as the first observable deviation from linearity in the experimental data. This approach is taken in this section.

The calculated yield load ply stresses in the columns under $\Delta T = -900^{\circ}$ F in tables V and VI include the residual stresses. The magnitude of the residual stress is obtained by subtracting corresponding stress values in columns under $\Delta T = 0^{\circ}$ F from those under $\Delta T = -900^{\circ}$ F. As can be easily verified, ply lamination residual stresses of 40 ksi and greater can be obtained in plies with orientation angles greater than 15° from the load direction. The transverse tensile and

intralaminar shear strengths of the unidirectional composite are about 14 ksi (table II, column 1). Therefore, these lamination residual stresses are about three times greater than the corresponding transverse tensile or intralaminar shear strengths. This means that the aluminum matrix is stressed beyond its yield point by the lamination residual stresses. This is consistent with the observation made previously with respect to the initial modulus values.

The calculated yield load ply stresses without residual stress are tabulated in the columns under $\Delta T = 0$, tables V and VI. Values for transverse and intralaminar shear stresses in these columns are relatively small when compared with the corresponding ply strengths in table II column 1. The point to be noted from these comparisons is that a load greater than the observed yield load would have been required to yield the specimens if the residual stresses had not been present.

The values in columns (F) under both $\Delta T = -900^{\circ}$ F and $\Delta T = 0^{\circ}$ F, tables V and VI are a measure of the ply combined stress yielding as predicted by the yield stress function (F).

The conditions for yielding under combined stress (3) are as follows:

$F > 0$ no yielding

$F = 0$ incipient yielding

$F < 0$ yielding occurred

Comparing corresponding F values under $\Delta T = -900^{\circ}$ F and $\Delta T = 0^{\circ}$ F, the following observations can be made:

1. The theoretical calculations indicate that most of the plies in specimens with ply orientation angles greater than 15° had yielded when the residual stress was combined with the applied yield load stress.

2. However, practically no ply had yielded in all the specimens when the residual stress was omitted from the theoretical calculations.

Three conclusions are made from the previous discussion:

1. The lamination residual stresses influence the yield load ply stress. The specimens actually yielded at a lower load than is pre-

dicted when the residual stresses are omitted.

2. The in situ ply yield stresses, in a combined stress condition, can be different from those observed for the unidirectional composite experimentally. This is a partial explanation for the large negative F values under $\Delta T = -900^{\circ}$ F.

3. Linear laminate theory predicts high residual stresses at room temperature. This is another partial explanation of the large negative F values under $\Delta T = -900^{\circ}$ F.

In Situ Ply Strengths of Boron/Aluminum Composites

An estimate on the in situ ply fracture stress is obtained by calculating the ply stresses at fracture load. These calculations for the specimens tested are summarized in the last three columns of tables V and VI. To calculate the ply stresses in these columns, it was assumed that no fiber breaks occurred prior to specimen fracture and there was no residual stress.

Examination of the theoretical stress values (tables V and VI), under column $\sigma_{\ell 11}$, shows that the in situ longitudinal tensile fracture stress could be as high as 263 ksi. A value of 263 ksi is about 40 percent greater than the corresponding experimental values from table II column 1. The following conclusions are drawn from this:

1. The theoretical in situ longitudinal tensile fracture stress is greater than the experimental stress in a unidirectional composite.

2. Nonlinear laminate theory would be required to obtain a better estimate.

Possible Factors Contributing to the Nonlinear Boron/Aluminum Composite Mechanical Behavior

The stress/strain curves (figs. 3 to 5) show considerable nonlinearity for some laminates. Several factors which may contribute to this

nonlinear behavior of boron/aluminum angleplied laminates are:

1. Nonlinear aluminum-matrix behavior (table II).
2. Fiber breaks prior to laminate fracture load as described by Prewo and Kreider (6).
3. Change of principal strain direction with increasing load (table VIII) including ply relative rotation (scissoring effect).

A nonlinear laminate theory to predict the nonlinear behavior of boron/aluminum angleplied laminates should include all of the above three factors. A theoretical capability accounting for these factors and at the micromechanics level would avoid the requirement for evaluating experimentally in the in situ ply nonlinear mechanical behavior. It is worthy of note that the computer code (4), which was used for the theoretical predictions in this investigation, can be readily extended to handle the nonlinear aspects in an incremental fashion.

SUMMARY OF RESULTS AND CONCLUSIONS

A combined experimental/theoretical investigation was conducted to study the mechanical behavior of angleplied boron/aluminum laminates. The experimental investigation consisted of determining the stress-strain behavior of various angleplied boron/aluminum laminates tested in tension along the laminate axis of symmetry and at some angles to this axis. The theoretical investigation consisted of using linear laminate theory, available in a computer code, to predict instantaneous initial and final elastic constants and also the "yield" and fracture lead ply stresses. The investigation led to the following results and conclusions:

1. The angleplied boron/aluminum laminates tested exhibited nonlinear stress-strain behavior.

2. The initial portion (up to "yield") of the stress-strain curve was limited to relatively small strains. These strains were about 12 percent of the corresponding fracture strains.

3. The fracture strain was approximately constant, about 0.7 percent, when the fiber direction in some plies was coincident with, or nearly coincident with, the load direction.

4. Lamination residual stresses strongly influence the initial portion (up to "yield") of the stress-strain curve.

5. The in situ ply longitudinal fracture stress, as calculated by linear composite mechanics, is 10 to 40 percent greater than that measured experimentally in unidirectional laminates from boron/aluminum composites.

6. Initial and final elastic constants, predicted by linear composite mechanics, are significantly higher than those observed experimentally.

7. Nonlinear composite mechanics is required to predict the mechanical behavior of angleplied boron/aluminum laminates.

8. Nonlinear mechanics should be based on the micromechanics level to avoid characterizing the mechanical behavior of individual plies under combined stress.

9. Nonlinear composite mechanics, for realistic predictions, should include matrix nonlinearity, possible fiber breaks before laminate fracture, and possible change of fiber direction with increasing load.

REFERENCES

1. Stuhrke, W. F., "The Mechanical Behavior of Aluminum-Boron Composite Material," Metal Matrix Composites, ASTM STP 438, 1968.

2. Swanson, G. D. and Hancock, J. R., "Off-Axis and Transverse Properties of Boron Reinforced Aluminum Alloys," Composite Materials: Testing and Design, ASTM STP 497, 1972.

3. Chamis, C. C., "Characterization and Design Mechanics for Fiber Reinforced Metals," NASA Technical Note D-5784, 1970.

4. Chamis, C. C., "Computer Code for the Analysis of Multilayered Fiber Composites-User's Manual," NASA Technical Note D-7013, 1971.

5. Chamis, C. C., "Lamination Residual Stresses in Multilayered Fiber Composites," NASA Technical Note D-6146, 1971.

6. Prewo, K. M. and Krieder, K. G., "High-Strength Boron and Borsic Fiber Reinforced Aluminum Compsoites," Journal of Composite Materials, Vol. 6, 1972, pp. 338-357.

TABLE I. - SUMMARY OF EXPERIMENTAL DATA

Laminate configuration	Load angle	σ_x (ksi)		Yield strains (10^{-3} in./in.)			Fracture strain (10^{-3} in./in.)			Modulus (10^6 psi)	
		"Yield[a]"	Fracture	ϵ_{xx}	ϵ_{yy}	ϵ_{xy}	ϵ_{xx}	ϵ_{yy}	ϵ_{xy}	Initial	Final
8(0)		30	180	0.80	-0.18	~0	6.5	-1.8	~0.15	33.8	22.3
$(0_2 \pm 5)_s$		30	200	.82	-.21	~0	7.4	-2.5	~.16	32.7	24.7
$(0_2 \pm 15)_s$	0	20	174	.76	-.17	-.03	6.9	-2.5	-.13	29.0	22.5
	+10	22	110	.83	-.23	-.27	6.7	-3.6	-9.4	26.0	12.4
	+15	23	91	.87	-.30	-.33	7.2	-4.6	-11.1	26.0	6.8
	-30	15	41	1.3	-.55	.94	12.8	-5.9	12.0	14.1	1.4
$(0_2 \pm 30)_s$	0	20	127	.86	-.28	~0	7.3	-5.6	~0	23.0	14.8
	+10	20	139	.95	-.36	-.16	8.7	-6.1	4.2	23.0	13.4
	-15	10	100	.39	-.12	.09	6.6	-3.8	3.5	24.0	13.6
	-30	14	64	1.1	-.39	.69	7.2	-1.3	7.2	16.0	6.8
$(0_2 \pm 45)_s$	0	12	99	.42	-.13	.02	6.1	-3.6	.03	22.0	13.4
$(0_2, 90_2)_s$	0	10	94	.42	-.05	~0	6.6	-6.2	.34	22.0	10.6

[a]First observed deviation from linearity.

TABLE II. - THEORETICAL VARIATION OF UNIDIRECTIONAL COMPOSITE LAMINATE OR PLY PROPERTIES WITH INSTANTANEOUS MATRIX MODULUS

Property	Units	Matrix modulus, psi				
		[a]10^7	10^6	10^5	10^4	10^3
$E_{\ell 11}$	10^6 psi	33.8	29.3	28.9	28.8	28.8
$E_{\ell 22}$	↓	21.0	2.6	.27	.03	.003
$G_{\ell 12}$	↓	7.2	.8	.08	.01	~0
$\nu_{\ell 12}$	↓	.25	.25	.27	.28	.31
$\alpha_{\ell 11}$	10^{-6} in./in./°F	3.3	2.9	2.8	2.8	2.8
$\alpha_{\ell 22}$	10^{-6} in./in./°F	10.7	11.0	11.3	11.4	11.7
$S_{\ell 11T}$	ksi	185	149	145	145	145
$S_{\ell 11C}$	↓	267	113	101	20	2
$S_{\ell 22T}$	↓	14.0	1.0	~0	~0	~0
$S_{\ell 22C}$	↓	25.7	1.8	~0	~0	~0
$S_{\ell 12S}$	↓	13.9	1.1	.1	~0	~0

[a]The values in this column were supplied by the fabricator.

TABLE III. - THEORETICAL ELASTIC CONSTANTS OF

THE BORON/ALUMINUM LAMINATES

[Fiber volume ratio = 0.5.]

Laminate configuration	Load angle	Initial, $E_m = 10^7$ psi				[a]Final, $E_m = 10^5$ psi			
		E^{b}_{cxx}	E_{cyy}	G_{cxy}	ν_{cxy}	E_{cxx}	E_{cyy}	G_{cxy}	ν_{cxy}
8(0)	0	33.8	21.0	6.9	0.251	28.8	0.28	0.08	0.274
$(0_2 \pm 5)_s$	0	33.6	20.9	7.0	.255	28.5	.28	.18	.663
$(0_2 \pm 15)_s$	0	32.5	20.6	7.5	.279	24.2	.30	.97	2.87
	+10	30.8	20.4	7.7	.299	15.4	.32	.76	.68
	+15	29.1	20.2	8.0	.319	10.0	.34	.60	-.405
	-30	23.7	19.6	9.4	.369	2.7	.50	.34	-.95
$(0_2 \pm 30)_s$	0	29.4	20.1	8.6	.331	16.0	.82	2.77	2.38
	+10	28.8	20.2	8.7	.332	16.2	.87	1.99	1.83
	-15	28.0	20.3	8.8	.333	15.7	.94	1.50	1.14
	-30	25.2	21.0	9.2	.329	8.1	1.43	.79	-.640
$(0_2 \pm 45)_s$	0	26.9	20.8	9.2	.341	14.6	3.10	3.66	.954
$(0_2, 90_2)_s$	0	27.4	27.4	6.9	.192	14.6	1.46	.08	.005

[a]Final refers to properties predicted at fracture load.

[b]E_{cxx}, E_{cyy} and G_{cxy} are in 10^6 psi.

E-7378

TABLE IV. - EXPERIMENTAL YIELD AND FRACTURE LOADS

FOR BORON/ALUMINUM TEST SPECIMENS

[Fiber volume ratio = 0.5.]

Laminate configuration	Load angle, deg	Thickness, in.	Load (lb)		Stress (ksi)	
			Yield	Fracture	Yield	Fracture
8(0)	0	0.0370	1110	6600	30	180
$(0_2, \pm 5)_s$	0	.0370	1110	7400	30	200
$(0_2 \pm 15)_s$	0	.0380	760	6612	20	174
	+10	↓	836	4180	22	110
	+15		874	3458	23	91
	-30	↓	570	1558	15	41
$(0_2 \pm 30)_s$	0	.0375	750	4762	20	127
	+10	↓	750	5212	20	139
	-15		375	3750	10	100
	-30	↓	525	2400	14	64
$(0_2 \pm 45)_s$	0	.0380	456	3762	12	99
$(0_2, 90_2)_s$	0	.0370	370	3478	10	94

TABLE V. - SUMMARY OF CALCULATED PLY STRESSES FOR SPECIMENS LOADED PARALLEL TO THE 0°-PLY DIRECTION

Laminate configuration	Ply in which stresses were calculated	Yield load ply stresses (ksi) for $E_m = 10^7$ psi								Fracture load ply stresses (ksi) $E_m = 10^5$ psi and $\Delta T = 0^{\circ}$ F		
		With residual stress ($\Delta T \approx -900^{\circ}$ F)				No residual stress ($\Delta T = 0^{\circ}$ F)						
		σ_{l11}	σ_{l22}	σ_{l12}	F	σ_{l11}	σ_{l22}	σ_{l12}	F	σ_{l11}	σ_{l22}	σ_{l12}
8(0)	0	30.0	0	0	0.974	30.0	0	0	0.974	178.4	0	0
$(0_2 \pm 5)_s$	0	30.2	.2	0	.975	30.1	~0	0	.973	202.0	0	0
	+5	28.4	1.2	-9.4	.515	29.9	~0	1.3	.965	199.5	-.7	.2
$(0_2 \pm 15)_s$	0	20.8	2.5	0	.986	20.5	-.4	0	.986	205.8	-5.2	0
	+15	6.2	10.5	-25.3	-4.251	19.2	.5	-2.7	.952	152.2	-4.8	-1.1
$(0_2 \pm 30)_s$	0	18.7	12.5	0	-1.990	22.7	-1.2	0	.976	227.3	-4.6	0
	+30	-31.1	39.9	-40.0	-30.69	16.0	2.5	-5.4		34.6	-3.3	-1.8
$(0_2 \pm 45)_s$	0	-6.2	33.6	0	-16.32	14.9	-.9	0	.989	194.7	-1.3	0
	+45	-74.8	71.4	-31.9	-76.88	6.0	4.0	-4.1	.601	4.5	~0	-1.0
$(0_2, 90_2)_s$	0	-60.3	73.2	0	-76.60	12.4	4.7	0	.996	186.2	.5	0
	90	-73.2	80.3	0	-91.73	-.5	7.6	0	.110	.5	1.8	0

E-7378

TABLE VI. - SUMMARY OF CALCULATED PLY STRESSES FOR SPECIMENS LOADED AT SOME ANGLE TO THE 0°-PLY DIRECTION

Laminate configuration and load angle	Ply at which stresses were calculated	Yield load ply stresses (ksi) for $E_m = 10^7$ psi								Fracture load ply stresses (ksi) $E_m = 10^5$ psi and $\Delta T = 0^{\circ}$ F		
		With residual stress ($\Delta T = -900^{\circ}$ F)				No residual stress ($\Delta T = 0^{\circ}$ F)						
		σ_{l11}	σ_{l22}	σ_{l12}	F	σ_{l11}	σ_{l22}	σ_{l12}	F	σ_{l11}	σ_{l22}	σ_{l12}
$(0_2 \pm 15)_s$	0	22.2	3.1	-3.5	0.916	22.1	0.3	-3.5	0.923	115.7	-1.7	-1.5
$\theta_{L/O} = 10^{\circ}$	+15	3.8	13.2	-28.4	-6.100	16.8	3.2	-5.8	.447	-34.4	.9	-1.5
	-15	11.3	9.1	22.4	-3.176	24.2	-.9	-.2	.925	243.6	-1.1	-1.1
$(0_2 \pm 15)_s$	0	22.3	4.0	-5.3	-2.806	22.2	1.2	-5.3	.838	81.1	3.0	-1.8
$\theta_{L/O} = 15$	+15	2.0	15.1	-29.8	-7.362	14.8	5.1	-7.2	.017	-73.1	4.1	-1.3
	-15	13.5	8.8	20.6	-2.763	26.4	-1.2	-2.0	.950	263.0	-1.7	-1.8
$(0_2 \pm 15)_s$	0	11.6	6.4	6.0	-.024	11.5	3.6	6.0	.427	3.9	8.4	1.4
$\theta_{L/O} = -30$	+15	4.6	10.3	-18.2	-2.498	17.5	.3	4.4	.889	193.1	7.0	2.4
	-15	-8.3	17.4	28.6	-7.858	4.6	7.4	6.0	-.104	-69.4	8.9	~0
$(0_2 \pm 30)_s$	0	17.0	13.2	-2.7	-2.276	21.9	-5.4	-2.7	.943	223.7	-3.5	.7
$\theta_{L/O} = 10^{\circ}$	+30	-36.5	43.1	-41.0	-34.83	10.6	5.7	-6.4	.116	-46.9	1.7	-1.9
	-30	-26.3	37.5	38.3	-27.38	20.8	.1	3.7	.916	167.3	-3.2	1.2
$(0_2 \pm 30)_s$	0	6.5	13.8	2.0	-2.172	10.5	.1	2.0	.976	138.9	-1.2	.7
$\theta_{L/O} = -15^{\circ}$	+30	-35.7	37.0	-35.9	-25.52	11.4	-.4	-1.3	.986	175.6	-1.5	-.4
	-30	-43.1	41.1	37.9	-30.74	3.9	3.7	3.3	.694	-49.7	.1	1.0
$(0_2 \pm 30)_s$	0	7.4	16.7	4.8	-3.682	11.5	3.0	4.8	.527	18.8	3.5	.8
$\theta_{L/O} = -30^{\circ}$	+30	-28.5	36.4	-33.8	-24.38	18.6	-.9	.9	.980	227.7	2.0	1.2
	-30	-46.6	46.4	38.6	-37.68	.5	9.0	4.0	-.359	-22.0	3.7	-.4

TABLE VII. - SUMMARY OF THEORETICAL AND EXPERIMENTAL VALUES FOR MODULUS AND POISSON'S RATIO OF BORON/ALUMINUM COMPOSITES

[Fiber volume ratio = 0.5.]

Laminate configuration	Load angle	Modulus in 10^6 psi				Poisson's ratio			
		Initial		Final		Initial		Final	
		Theoretical	Experimental	Theoretical[a]	Experimental	Theoretical	Experimental	Theoretical	Experimental
8(0)	0	33.8	33.8	28.8	22.3	0.237	0.222	0.274	0.252
$(0_2 \pm 5)_s$	0	33.6	32.7	28.5	24.7	.255	.258	.663	.426
$(0_2 \pm 15)_s$	0	32.5	29.5	24.2	22.5	.279	.245	2.87	.415
	+10	30.8	26.0	15.4	12.4	.299	.304	.68	.593
	+15	29.1	26.0	10.0	6.8	.319	.293	-.405	.658
	-30	23.7	14.1	2.7	1.4	.369	.335	-.95	.583
$(0_2 \pm 30)_s$	0	29.4	23.0	16.0	14.8	.331	.326	2.38	1.84
	+10	28.5	23.0	16.2	13.4	.332	.369	1.83	.872
	-15	28.0	24.0	15.7	13.6	.333	.383	1.14	.646
	-30	25.2	16.0	8.1	6.8	.329	.343	-.640	-.20
$(0_2 \pm 45)_s$	0	26.9	22.0	14.6	13.4	.341	.356	.954	.677
$(0_2, 90_2)_s$	0	27.4	22.0	14.6	10.6	.192	.107	-.005	.104

[a]Final theoretical values were based on $E_m = 10^5$ psi.

E-7378

TABLE VIII. - DIRECTION OF STRAIN PRINCIPAL AXES

Laminate configuration	Load angle, deg		
	Load direction	First load increment	Fracture load
8(0)	0	0.30	0.65
$(0_2 \pm 5)_s$	0	-.27	.47
$(0_2 \pm 15)_s$	0	0	
	+10	-5.24	-21.19
	+15	-6.97	-22.27
	-30	11.22	15.96
$(0_2 \pm 30)_s$	0	-.81	-2.42
	+10	-1.92	-7.91
	-15	5.13	9.33
	-30	10.62	20.29
$(0_2 \pm 45)_s$	0	.96	.08
$(0_2, 90_2)_s$	0	-.14	1.34

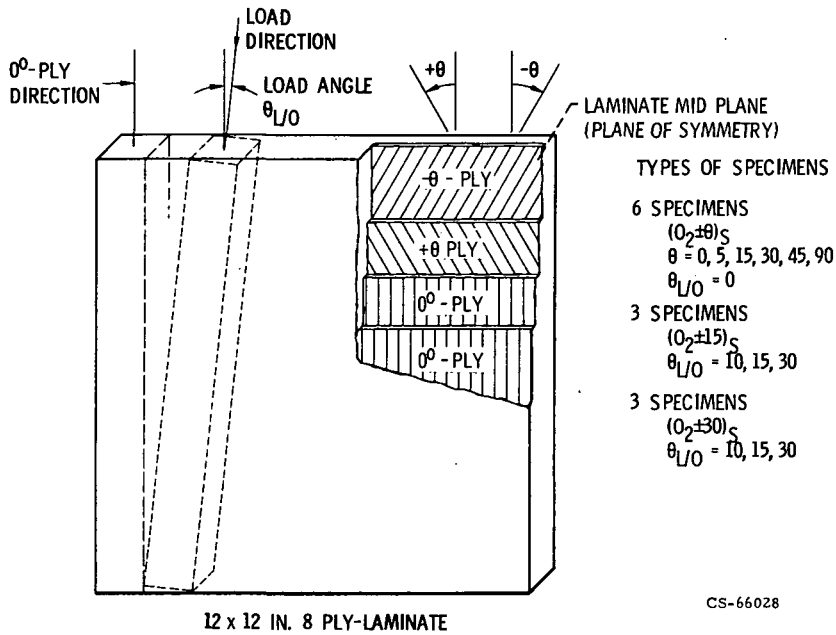

Figure 1. - Laminate geometry and types of specimens.

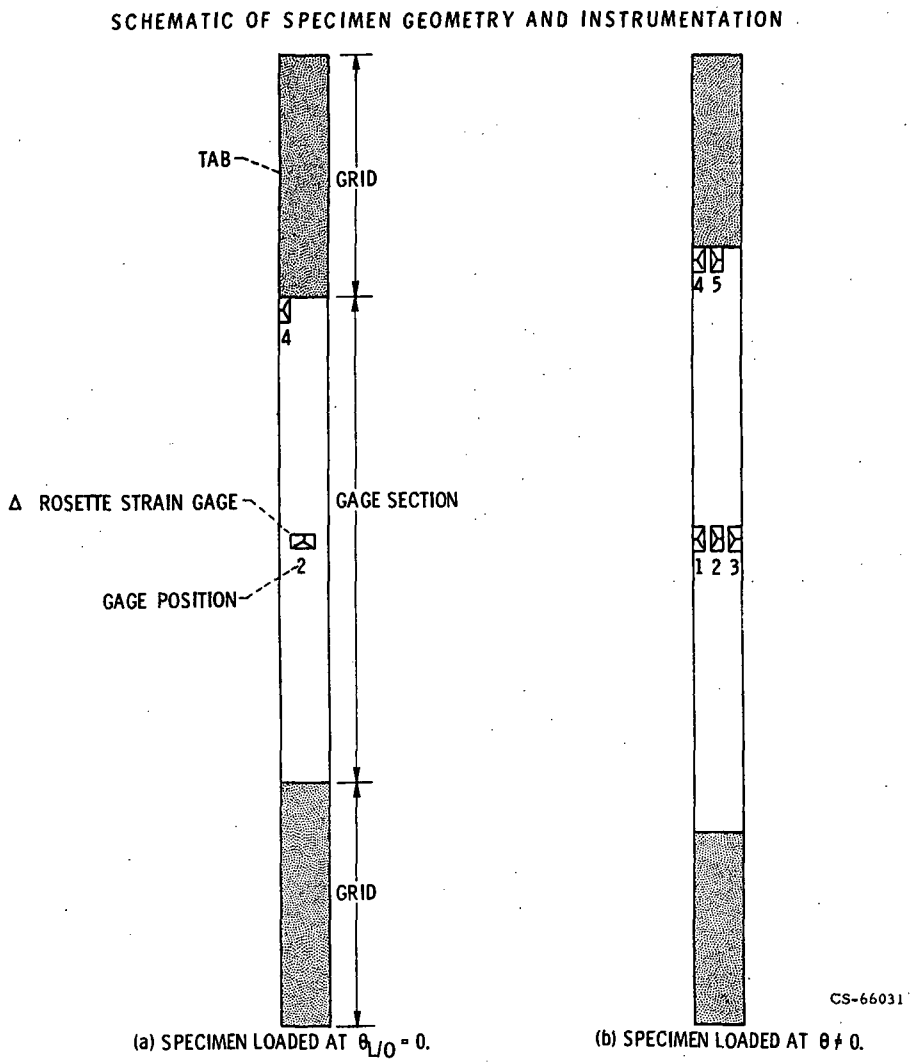

Figure 2. - Schematic of specimen geometry and strain gage arrangement.

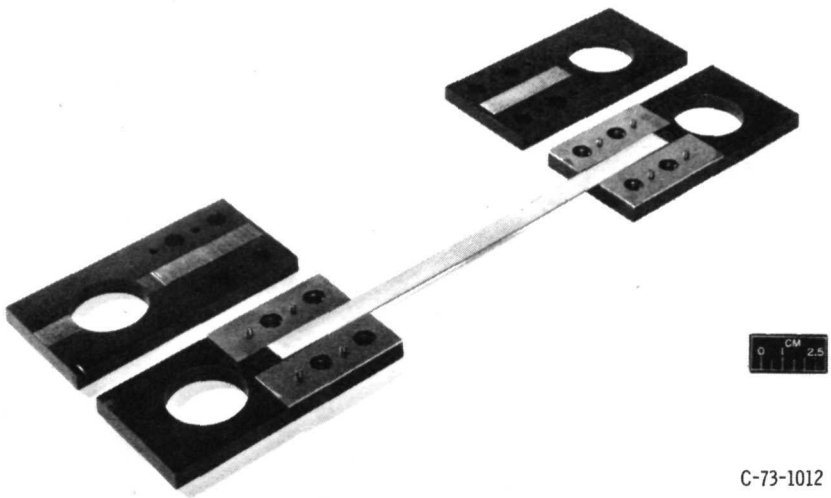

C-73-1012

(a) GRIPS DISASSEMBLED.

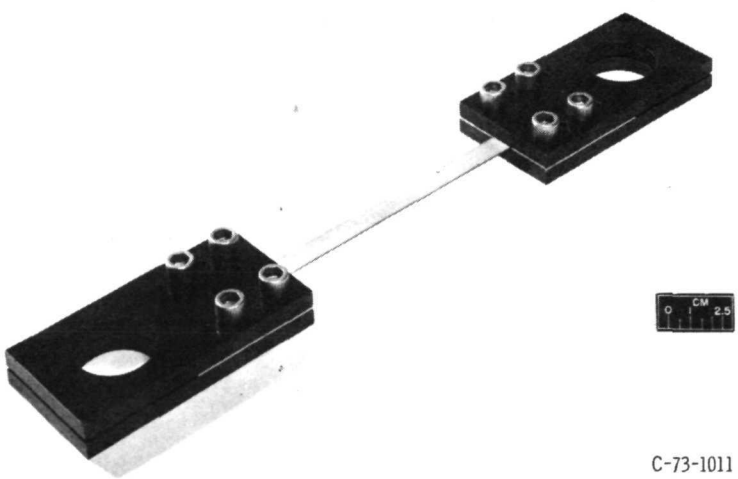

C-73-1011

(b) GRIPS ASSEMBLED.

Figure 3. - Boron/aluminum composite coupon grips.

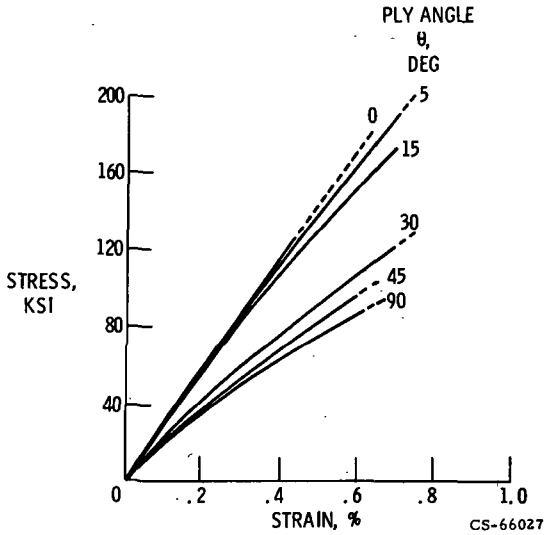

Figure 4. - Experimental stress-strain curves of boron/aluminum laminates $(0_2 \pm \theta)_S$ loaded parallel to the 0^0 ply direction. (Fiber volume ratio ≈ 0.50.)

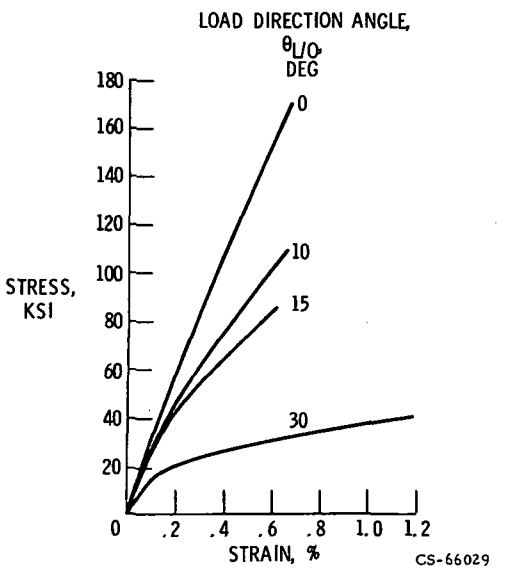

Figure 5. - Experimental stress-strain curves of boron/aluminum laminates $(0_2 \pm 15)_S$ tested at various angles to 0^0 ply direction. (Fiber volume ratio ≈ 0.5.)

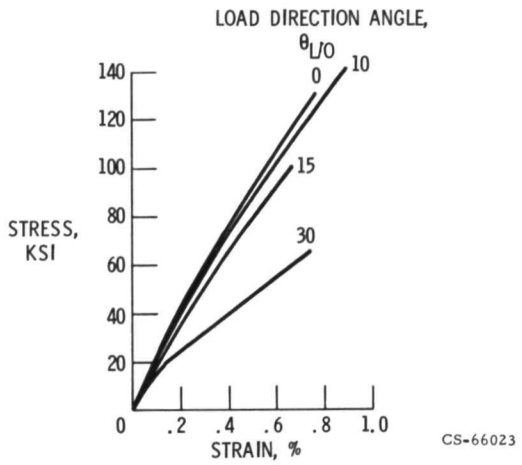

Figure 6. - Experimental stress-strain curves of boron/aluminum laminates $(0_2 \pm 30)_S$ tested at various angles to the 0^o ply direction. (Fiber volume ratio ≈ 0.5.)

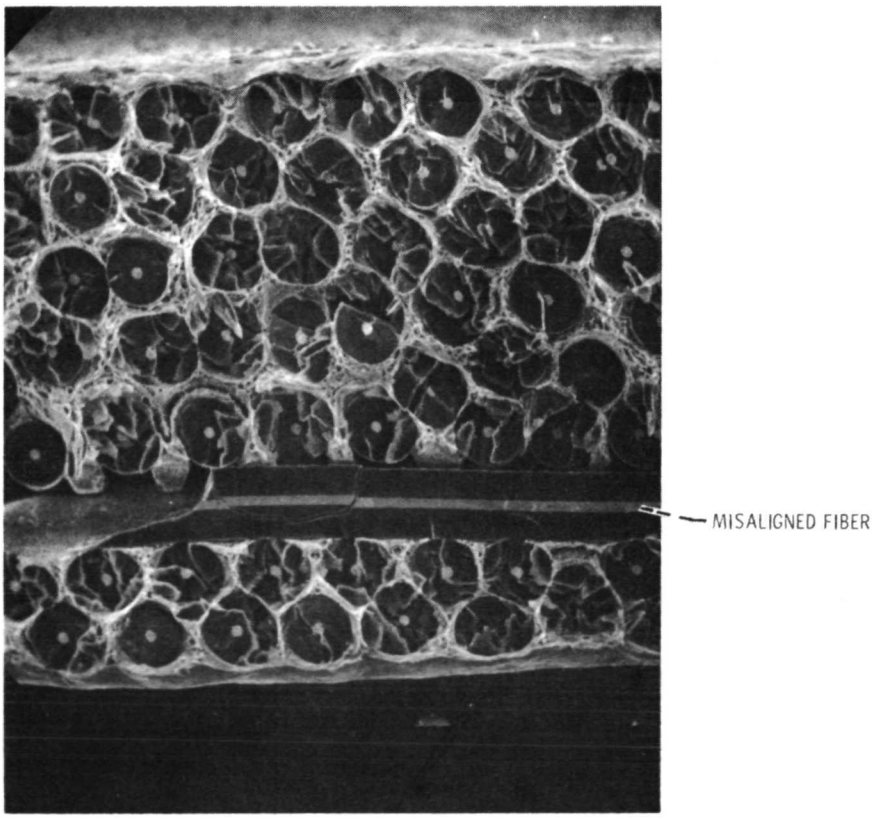

Figure 7. - Photomicrograph of fracture surface showing misaligned fiber in the unidirectional laminate.